PHOTOVOLTAIC HEAT PUMP SYSTEM FOR RENOVATED BUILDINGS – MEASURES FOR INCREASED EFFICIENCY

Andreas Heinz[1], Christian Gaber[1], Robert Haberl[2], Michel Y. Haller[2], Joachim Kalkgruber[3] and Rüdiger Schober[3]

[1] Institute of Thermal Engineering (IWT), Graz University of Technology, 8010 Graz (Austria)

[2] SPF Institute for Solar Technology, Eastern Switzerland University of Applied Sciences (OST), Rapperswil (Switzerland)

[3] SOLARFOCUS GmbH, St.Ulrich/Steyr (Austria)

Abstract

In this paper we describe the development and analysis of a hybrid heating system for space heating and domestic hot water that is designed to enable an energy-efficient supply of renovated residential buildings with an existing radiator heating system, requiring high flow temperatures. The system consists of a dedicated air-to-water heat pump using the natural refrigerant R290 (Propane), a thermal energy storage, a photovoltaic system and an advanced control. The development is done with the objective of a reduction of the system's electrical energy consumption from the grid by 25 % compared to a defined reference system. Detailed system simulations in TRNSYS were performed to evaluate the effect of different measures concerning the heat pump cycle, the storage tank and the control for a renovated reference single family house. The results show that with a combination of all considered measures a reduction of the grid consumption by 32 % compared to the reference system is possible with a PV size of 10 kWp. With 5 kWp still a reduction of 25 % can be achieved.

Keywords: Air-to-water heat pump, photovoltaic, self-sufficiency

1 Introduction

The building sector plays a central role in achieving energy and climate policy objectives all over Europe. In Austria more than one third of the final energy consumption is used to provide space heating, domestic hot water and cooling in residential and service buildings. With a construction rate of new buildings of only about 1-2 % per year, the greatest energy saving potential lies with existing buildings in need of renovation. Around 1.5 million of the 2 million buildings in Austria fall into the single-family or two-family house category, providing a large potential for savings. With regard to the construction periods, the highest potential lies with buildings built between 1961 and 1980, since about one third of the entire Austrian building stock was constructed in this period (Amtmann, 2010).

Thermal renovation together with the replacement of inefficient, fossil fuel based heating systems provides a large potential for energy savings. Air-to-water heat pumps are in principle an attractive alternative heating system for such buildings due to relatively low investment costs and simple installation. However, this solution is often not implemented due to the heat emission system, which usually consists of radiators, that are often not replaced during a renovation because of cost reasons. Therefore, relatively high supply temperatures are required, which limits the efficiency of the heat pump (HP).

In the last years the demand for solutions enabling a high self-consumption of electricity from PV plants has strongly increased due to the decrease of feed-in tariffs for electricity from photovoltaic (PV) systems and as possibility for stabilizing the electricity grid. Strategies for increasing PV self-consumption for heating systems with heat pumps have recently been analyzed with system simulations in (Battaglia et al., 2017) for an air source heat pump, in (Thür et al., 2018) for a ground source heat pump system, and in (Toradmal et al., 2018) for an air- and ground source heat pump, all of them reporting promising results.

In this paper we describe and analyze a hybrid heating system for space heating and domestic hot water that is

doi:10.18086/eurosun.2020.04.01 Available at http://proceedings.ises.org

developed in the ongoing research project “HybridHeat4San”. The system is designed to enable an energy-efficient supply of renovated residential buildings with an existing radiator heating system, requiring high flow temperatures. A reduction of the overall electricity consumption is achieved by an efficient air-source heat pump and an optimized integration of a water combi storage tank (combistore). The HP is coupled to a PV system with the aim to reduce the electricity consumed from the grid by targeted operation of the compressor with PV electricity using an intelligent control strategy.

The described system is analyzed using detailed system simulations in TRNSYS 17 (2014) and results are compared to a defined reference system using a set of performance indicators. Different control strategies are evaluated concerning the fulfillment of the project objective, which is to reach a reduction of electricity consumption from the grid of 25 % compared to the reference system. The influence of the PV size on performance figures and the operational (electricity) costs is analyzed.

2 Boundary conditions and assumptions

2.1 Building, climate and domestic hot water

A single-family house with a heated floor area of 185 m² was defined as the reference building (Fig. 1) in two variants concerning the thermal insulation standard and was modelled in the simulation software TRNSYS 17:

- Before renovation
- After renovation (usual renovation)

The wall structures were chosen on the basis of building typologies for Austria defined in the European project TABULA (Tabula, 2018). The starting point was a building of the age class 1960-1981 with the according wall structures as defined in TABULA, which defines the variant “before renovation”. For the “after renovation” scenario, a “usual renovation”, like it is defined in TABULA with according wall structures, was used.

All assumptions regarding the air exchange (incl. additional window ventilation in summer) and the shading of the building were taken from the reference building model of the IEA SHC Task 44 (Dott et al., 2013). The software "Load Profile Generator" (2018), which was developed as part of a dissertation at Chemnitz University of Technology (Pflugradt, 2016), was used for the internal heat gains from devices and lighting as well as from persons present in the building. Load profiles were created for a household with four persons (both parents working, two school-aged children) stored as a template in the software. For the heat gains by devices and for the presence of persons, a separate load file for the TRNSYS simulation was created.

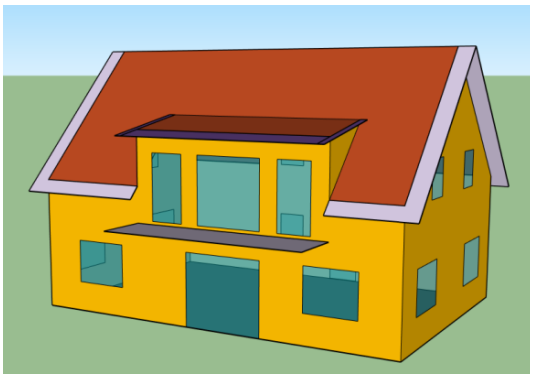

Fig. 1: Reference single family building

The resulting load profile for devices and lighting was created with a resolution of one minute and results in electrical gains totaling 16.4 kWh/m².a. The same profile is also assumed for the consumption of household electricity with a total of 3058 kWh/a. For the persons present, a sensitive heat output of 60 W per person and a latent heat output of 40 W were assumed according to ISO 7730.

As climate data set a "Test Reference Year", as described in (Bales et al., 2012), for the city of Zurich is used. The annual average of the outdoor temperature is 9.1 °C, the solar radiation on a 45° inclined surface facing south sums up to 1306 kWh/(m².a) and to 1111 kWh/(m².a) on the horizontal.

Assuming a room set temperature of 22 °C the simulations resulted in a space heating demand of 38 670 kWh and a heat load of 15.4 kW for the building before renovation and 12 212 kWh/a and 7 kW after renovation. For all the simulations shown in this work the renovated building scenario was used.

The tap profile for domestic hot water (DHW) was taken from the FP7 project MacSheep (Bales et al., 2012). The profile was created with the DHW_{calc} software (Jordan and Vajen, 2012) and has a total heat demand of 3038 kWh.

2.2 Heat emission system

For the heat emission system, radiators with a radiator exponent n=1.3 were assumed. For the “before renovation” scenario, a flow temperature t_{fl}=90 °C and a return temperature t_{ret}=70 °C were assumed for the heating load $\dot{Q}_{100}$ in the design point (design ambient temperature -11 °C), which was still common for heating systems built in the 1960s and 70s according to (Biberacher, 2010) and (Schramek and Recknagel, 2007). For the "after renovation" scenario, the necessary t_{fl} and t_{ret} were determined for the reduced heating load of the renovated building assuming constant heating surfaces. Thus, at - 11 °C, the flow temperature is 58 °C and the return temperature 48.9 °C (see Fig. 2).

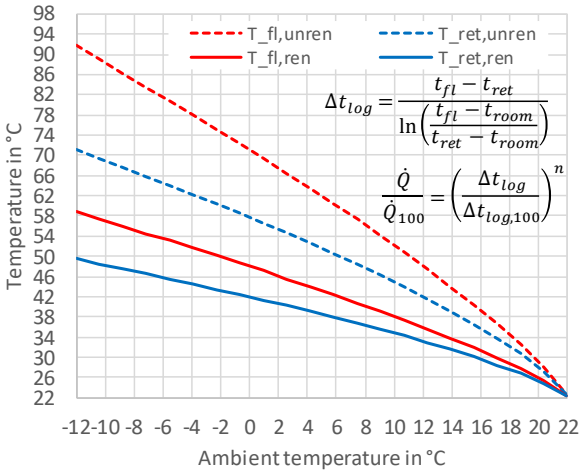

Fig. 2: Flow and return temperatures for the renovated (ren) and unrenovated (unren) building scenario

2.3 Hydraulic system layout

Regarding the system layout, two different variants were assumed. The first step in the project was to define a reference system that represented the current state of the art of HP systems available from the industrial partner in the project. This system was used as a basis for comparison to evaluate different measures of improvement for the System developed in the project (System B).

System A, depicted in Fig. 3, was used as the reference system. Here the DHW is heated in a hot water tank with a volume of 300 liters, which is charged via an internal heat exchanger. A buffer tank with a volume of 200 liters is connected in parallel to the heat emission system.

The air-source heat pump can charge one of the two storage tanks at a time, switching over via 3-way valves. The buffer storage tank is connected to the heat pump in parallel with the heating circuit. This means that when the heat pump charges the storage tank, part of the volume flow available in the heat pump circuit flows through the heating circuit. The proportion depends on the current flow rate in the heating circuit, which in turn depends on the current position of the three-way valve and the flow rate through the radiators.

For the heat losses of the storage tanks, it was assumed that the buffer tank has a heat loss value UA of 1.67 W/K and the hot water tank of 1.53 W/K, which corresponds to energy efficiency class C or B according to (EC, 2013).

System B, which was used as the basis for the system development within the project, is shown Fig.4. The air-source HP is connected to a storage tank with a volume of 1000 liters. The heat losses of the tank were assumed with efficiency class B according to (EC, 2013). Compared to the reference system the volume is larger, in order to provide storage capacity for the control strategies to increase PV self-consumption by targeted operation of the compressor to overcharge the storage (see section 2.7).

Using three-way-valves, the heat pump can charge either the DHW zone of the tank via the two connections on the top or the space heating zone via the lower connections. The storage tank is connected to the heat pump in parallel to the space heating system. This means, when the store is being charged for space heating by the heat pump, some of the flow will go via the space heating distribution loop and the rest will go through the store. As in the reference system, the proportions depend on the current operating conditions (current flow) of the space heating loop. DHW preparation is done via a freshwater station (external plate heat exchanger) to a temperature of 45 °C.

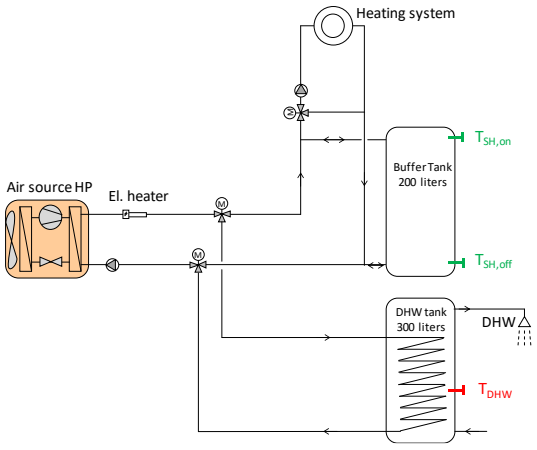

Fig. 3: Hydraulic layout of the reference heating system (System A)

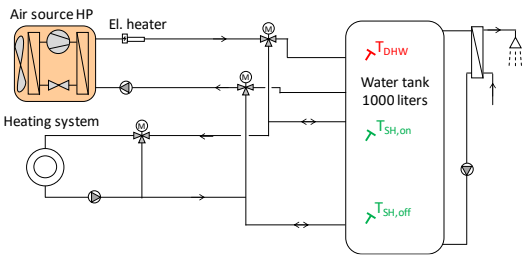

Fig. 4: Hydraulic layout of the developed heating system with combistore (System B)

2.4 Heat pump

The heat pumps of the two systems were modelled with the semi-physical HP model Type 887, which was developed by IWT and SPF (described in (Dott et al., 2013) and (Hengel et al., 2014)). The model is based on an iterative calculation of the refrigerant cycle using the thermodynamic properties of the used refrigerant. Start/stop losses and defrosting losses are considered. Detailed compressor performance data of real compressors was used, depending on the evaporation, condensation temperature and the compressor speed. The operational limits of the compressors were taken into account (max. condensation and min. evaporation temperature depending on the compressor speed).

Tab. 1: COP of the R410A HP model used for the reference system in comparison to test results from (NTB Buchs, 2018)

	A7/W35-30	A-10/W35	A-7/W34	A2/W35	A7/W27	A7/W55-47	A-10/W55	A-7/W52	A2/W42	A7/W36
Model HP Reference System	**4.52**	**2.72**	**3.02**	**3.77**	**5.48**	**2.95**	**2.04**	**2.26**	**3.24**	**4.34**
Test results Avg.	**4.71**	**2.62**	**2.80**	**3.76**	**5.60**	**2.83**	**1.94**	**2.14**	**3.19**	**4.56**
Test results Max.	5.10	3.20	3.30	4.30	6.70	3.30	2.30	2.40	3.80	5.10
Test results Min.	4.10	2.30	2.40	3.10	4.60	2.20	1.70	1.90	2.70	4.00
Deviation from test results Avg. in %	**-4.1**	**3.7**	**8.0**	**0.1**	**-2.1**	**4.1**	**5.2**	**5.8**	**1.5**	**-4.8**
Deviation from test results Max. in %	-11.4	-15.1	-8.3	-12.4	-18.2	-10.7	-11.3	-5.6	-14.8	-14.9
Deviation from test results Min. in %	10.2	18.2	26.0	21.5	19.2	33.9	20.1	19.2	19.9	8.5

For the reference system (**System A**) an air-to-water HP with a standard cycle (see Fig. 5) with accumulator and R410A as refrigerant was assumed. A speed controlled compressor with a speed range is 22 – 100 % used. The parameterized heat pump model results in a thermal capacity of 7.7 kW and a COP of 2.72 at the operating conditions A-10W35 and 10.8 kW and COP 3.39 at A2W35, both at full compressor speed.

Simulation results with the parameterized model were compared with test results for air-source heat pumps from a HP test center (NTB Buchs, 2018). An average of the COP results of all tested units with the refrigerant R410A and a heat output of up to 15 kW was determined for different operating conditions. In Table 1, the COP values resulting from simulations are compared with those of the test results. It can be seen that for all considered operating points, the simulation results are between the best and worst test results and mostly higher than average.

For **System B** a heat pump cycle with the natural refrigerant R290 (propane) was used. Propane offers superior properties especially concerning the compressor discharge temperature, which enables higher condensation temperatures and generally wider operational limits of the compressor. This offers advantages for the here discussed system with high flow temperatures and especially for the coupling with PV and overcharging to higher temperatures. The compressor used for this HP has a speed range of 17 to 100 %.

Additionally, a subcooler is used in the refrigerant cycle, which offers advantages concerning the COP, especially if the temperature difference on the heat sink side is large, as it is in the case of a radiator heating system. An exemplary operating point is shown in Fig. 5 in a temperature-enthalpy diagram for a standard cycle and a cycle

with additional subcooler. Simulations have shown that the subcooler improves the COP compared to a standard HP cycle without any subcooling by 4-7 % over the whole range of operating conditions.

A prototype of this HP was built by the industrial partner and measurements were carried out in the climate chamber of IWT. In total 50 different steady-state operating conditions[1] were measured, including defrosting cycles and an analysis of start/stop losses. The HP model used for the simulations of System B was parameterized using these measurements. The parameterized model results in a thermal capacity of 7.6 kW and a COP of 2.92 at the operating conditions A-10W35 and 10.2 kW and COP 3.82 at A2W35, both at full compressor speed.

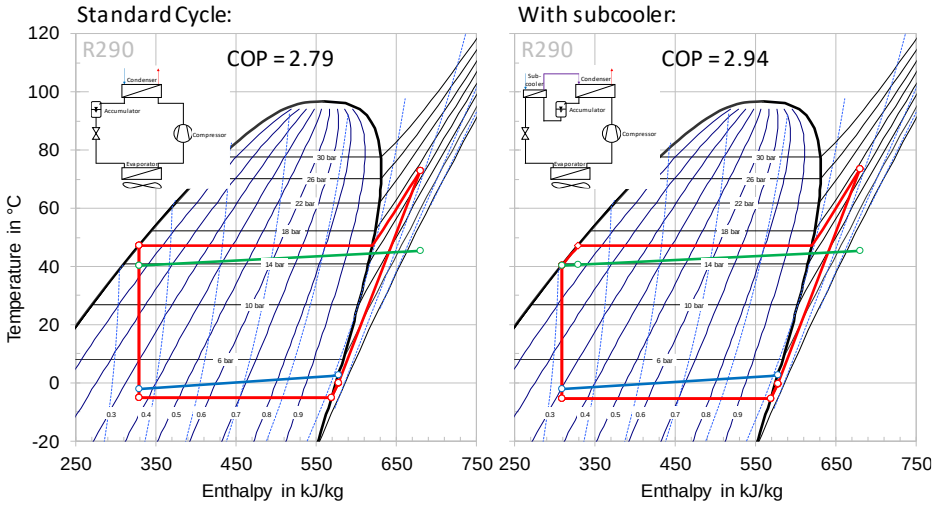

Fig. 5: T/h-diagram of an exemplary heat pump cycle with R290 @ A2W45 without (left) and with (right) subcooler

2.5 Storage tank

The combistore used in System B was optimized concerning the position of the inlets and outlets and of the temperature sensors by means of system simulations based on an initial configuration. For this purpose, the individual connection heights and sensor positions were varied in a large number of annual simulations within a certain range until and an optimum was found with regard to energy consumption.

Installations in the storage tank for efficient handling of the high volume flow rates of a heat pump to avoid inlet jet mixing were designed and selected using CFD simulations by the project partner SPF. The CFD simulations were carried out to find a suitable design for these diffusers. A total of 9 different geometries were simulated and their stratification behavior examined with simulations of both, hot water charging as well as the charging and discharging of the space heating zone.

The storage that was designed with the help of simulations was then tested on the test bench of SPF in dynamic operation, including the fresh water module for DHW preparation. A test method to measure the stratification efficiency as key performance indicator was used (Haller et al. 2018, Haller et al. 2019). The laboratory test is based on a 24-hour cycle, where realistic and dynamic charging and discharging is applied according to boundary conditions of real weather data of a day in the year. This work and the CFD optimization is described in detail in a second contribution to the EUROSUN 2020 conference by Haberl et al. (2020).

Based on the results of the 24-hour test the simulation models used for the annual TRNSYS simulations were parameterized. The storage tank was simulated using the one-dimensional multi-node model Type 340 (Drück, 2006), the fresh water module using Type 805 (Haller, 2007).

2.6 Photovoltaic system

For the photovoltaic panels the parameters of polycrystalline modules were used. The PV array was modelled using Type94a, based on the four-parameter equivalent circuit model (TRNSYS 17, 2014). The PV yield was calculated in every time step depending on the current solar radiation (diffuse and beam) and its incident angle

[1] Compressor speed range: 1700 to 7200 rpm,
heat source (air) temperatures: -10 to 12 °C,
heat sink temperatures: 35 to 65 °C

onto the PV panels. The efficiency of the inverter was assumed to be 0.94. In the basic variant of the system a PV size of 10 kWp is used, which is about the maximum that can be placed on the available roof area. A variation of the PV size is discussed later in the results section.

2.7 Control strategies

Concerning the control of the system three strategies are analyzed and compared:

- **Standard**: This is the basic control strategy that was used in System A and B for charging the storage tank(s). PV is only used by the heat pump if it is in operation by coincidence, when PV electricity is available. Charging of the DHW zone of the tank by the heat pump is started, if $T_{DHW} < 45$ °C (sensor position in Fig. 3 and Fig. 4) and is stopped, when $T_{DHW} > 55$ °C. The space heating zone is charged, if $T_{SH,on} < T_{fl}$ and stopped when $T_{SH,off} > T_{fl}+2K$, where T_{fl} is the flow temperature depending on the ambient temperature (Fig. 2).
- **PV_{Store}**: In this strategy, that was applied for System B in order to increase self-consumption and self-sufficiency (see section 3), the heat pump is used to overcharge the storage tank, when enough excess PV electricity is available. Whenever the available PV electricity exceeds the current household electricity demand by 0.7 kW the system is switched to "overcharging mode". This means that the DHW and space heating zone of the combistore are both heated to higher temperatures compared to strategy "Standard". Due to the operational limits of the compressor, overheating is done dependent on the ambient temperature (T_{amb}) to max. 60 °C when $T_{amb} > 5$ °C and to 55 °C if $T_{amb} \leq 5$ °C. In this mode, the speed of the compressor is adapted in order to match the electricity consumption of the heat pump to the available PV excess electricity ($P_{el,PV,exc}$, Eq.1). Overcharging is stopped when either the storage temperature reaches the temperature limit or PV excess drops below 0.6 kW.
- **PV_{Store} & PV_{Troom}**: For System B in addition to "PV_{Store}" the strategy "PV_{Troom}" makes use of the thermal inertia of the building structure. If the "overcharging mode" is active as described above, the set room temperature is increased by +0.5 K and otherwise decreased by -0.5 K, starting from the standard value of 22 °C. The basic idea is to shift heat generation into times with PV yield and to store heat in the building structure.

3 Performance figures

In order to enable a comparison of the analyzed variants of the system and the control the following performance figures were defined, all of them on an annual basis. The electricity consumption for the considered heating system ($W_{el,sys}$, Eq. 2) was calculated including the HP, pumps and the electrical heater. The energy that has to be drawn from the grid was determined both for the heating system ($W_{el,sys,grid}$, Eq. 3) and the whole building ($W_{el,grid}$, Eq. 4), including household (hh) electricity. This was done based on the time-step of one minute that was used in all simulations.

Three seasonal performance factors were determined. SPF_{HP} describes the performance of the HP as a component. The whole heating system was considered with SPF_{sys}, where only useful energy delivered for space heating (SH) and DHW was considered and the total electricity consumption of the system. Only taking into account the system's electricity consumption from the grid results in $SPF_{sys,PV}$.

The self-sufficiency ratio is the fraction of the electricity consumption that can be covered by PV and was calculated on the level of the heating system (SSR_{sys}) and for the whole building (SSR_{tot}) including household electricity. The fraction of PV electricity that is consumed on-site is expressed by the self-consumption ratio (SCR).

$$P_{el,PV,exc} = max\left(\left(P_{el,PV} - P_{el,hh}\right), 0\right) \quad \text{Eq. 1}$$

$$W_{el,sys} = \int \left(P_{el,HP} + P_{el,pumps} + P_{el,heater}\right) dt \quad \text{Eq. 2}$$

$$W_{el,sys,grid} = \int max\left(\left(P_{el,sys} - P_{el,PV,exc}\right), 0\right) dt \quad \text{Eq. 3}$$

$$W_{el,grid} = \int max\left(\left(P_{el,sys} + P_{el,hh} - P_{el,PV}\right), 0\right) dt \quad \text{Eq. 4}$$

$$W_{el,feedin} = \int max\left(\left(P_{el,PV,exc} - P_{el,sys}\right), 0\right) dt \quad \text{Eq. 5}$$

$$SPF_{HP} = \frac{\int \dot{Q}_{cond} dt}{W_{el,HP}} \quad \text{Eq. 6}$$

$$SPF_{sys} = \frac{\int \left(\dot{Q}_{SH} + \dot{Q}_{DHW}\right) dt}{W_{el,sys}} \quad \text{Eq. 7}$$

$$SPF_{sys,PV} = \frac{\int \left(\dot{Q}_{SH} + \dot{Q}_{DHW}\right) dt}{W_{el,sys,grid}} \quad \text{Eq. 8}$$

$$SSR_{sys} = 1 - \frac{W_{el,sys,grid}}{W_{el,sys}} \quad \text{Eq. 9}$$

$$SSR_{tot} = 1 - \frac{W_{el,grid}}{W_{el,sys} + W_{el,hh}} \quad \text{Eq. 10}$$

$$SCR = 1 - \frac{W_{el,feedin}}{W_{el,PV}} \quad \text{Eq. 11}$$

$$Net\ el.\ Costs = W_{el,grid}\ \ c_{Purchase} - W_{el,feedin}\ \ c_{feedin} \quad \text{Eq. 12}$$

The net electricity costs (Eq. 12) were calculated considering the total electricity consumption from the grid including household electricity ($W_{el,grid}$) and the amount of PV electricity sold to the grid ($W_{el,feedin}$). For the results shown in this paper an electricity purchase price $c_{purchase}$ of 0.18 €/kWh was assumed and a feed-in tariff c_{feedin} of 0.05 €/kWh, which currently are typical values in Austria.

4 Results and discussion

The simulation results are summarized in Table 2 for the systems A and B in form of the defined performance figures. System A, which was simulated only with the control strategy "Standard", was used as the reference case within the project with the objective of saving 25 % of electricity drawn from the grid ($W_{el,sys,grid}$). Simulations for System B were carried out with the three control strategies described in section 2.7.

Tab. 2: Performance figures for the simulated systems and control variants, difference compared to the reference system (System A) is indicated in brackets

System		System A (Reference system)	System B		
Control		**Standard**	**Standard**	**PV$_{Store}$**	**PV$_{Store}$ & PV$_{Troom}$**
$W_{el,sys}$	kWh/a	6726	5919 (-12.0 %)	6367 (-5.3 %)	6242 (-7.2 %)
$W_{el,sys,grid}$	kWh/a	5807	5032 (-13.3 %)	4359 (-24.9 %)	3964 (-31.7 %)
$W_{el,grid}$	kWh/a	7902	7127 (-9.8 %)	6454 (-18.3 %)	6059 (-23.3 %)
$W_{el,feedin}$	kWh/a	6877	6909 (+0.5 %)	5788 (-15.8 %)	5518 (-19.8 %)
SPF_{HP}	-	2.71	2.99 (+10.6 %)	2.86 (+5.6 %)	2.90 (+7.2 %)
SPF_{sys}	-	2.27	2.57 (+13.2 %)	2.39 (+5.3 %)	2.43 (+6.8 %)
$SPF_{sys,PV}$	-	2.63	3.02 (+14.9 %)	3.49 (+32.8 %)	3.82 (+45.2 %)
SSR_{sys}	-	0.19	0.21 (+7.1 %)	0.32 (+63.9 %)	0.35 (+81.1 %)
SSR_{tot}	-	0.14	0.15 (+9.6 %)	0.32 (+131 %)	0.36 (+167 %)
SCR	-	0.21	0.21 (-1.7 %)	0.34 (+57.9 %)	0.37 (+72.2 %)
Net el. Costs	€/a	1078	937 (-13.1 %)	872 (-19.1 %)	815 (-24.5 %)

Applying the control "Standard" both for System A and System B shows that the improved HP and storage setup results in a reduction of the system electricity consumption ($W_{el,sys}$) of 12 % and that 13 % less electricity has to be drawn from the grid ($W_{el,sys,grid}$). Detailed energy balances of the heating system for the simulated variants

are shown in Fig. 6. Compared to the reference, system SPF_{HP} is increased by 10 % (Table 2) due to better overall efficiency of the R290 cycle with the subcooler, although the HP losses of the prototype configuration are higher than what was assumed for the HP of the reference system (Fig. 6). Storage losses are reduced by about 200 kWh despite of the two times larger volume, due to slightly better insulation and better surface area to volume ratio of one large store compared to two small ones.

Electrical energy balances including household electricity are shown in Fig. 7. A fraction of 31 % of the household electricity can be covered by PV in all considered variants. This is independent of the used control strategies, as they only influence the heating system and not the household electricity consumption.

With the control "Standard" and the assumed PV size of 10 kWp, a system self-sufficiency ratio SSR_{sys} of 19 % is achieved for System A, whereas System B reaches 21 %. This is mainly due to the lower energy consumption $W_{el,sys}$. The net electricity costs are 13 % lower for System B compared to System A due to lower electricity consumption from and slightly higher feed-in into the grid.

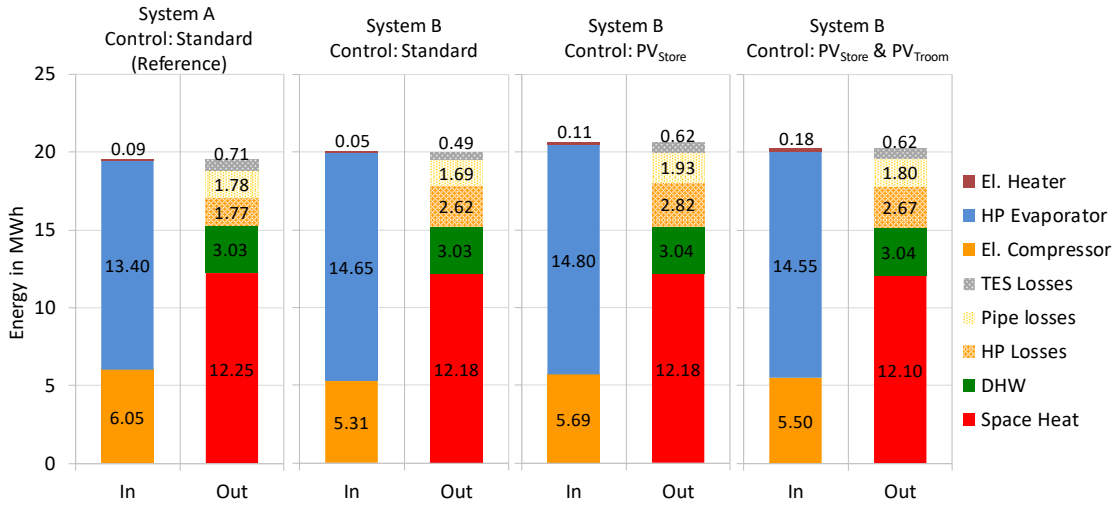

Fig. 6: Energy balance for System A and System B with different control strategies; Energy flow into the system is shown on the left (In), energy consumption and losses on the right (Out)

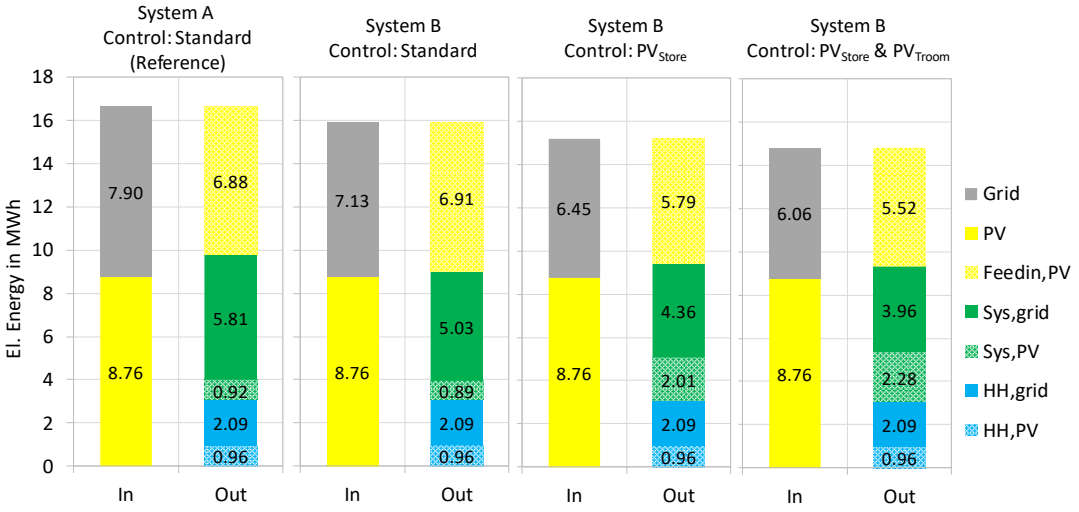

Fig. 7: Electrical energy balance for System A and System B with different control strategies

Applying control strategy "PV_{Store}" to System B results in a reduction of SPF_{HP} and increased electricity consumption of the system $W_{el,sys}$. This is due to the HP being increasingly operated with higher condensation temperatures, when overheating of the store is performed in times of available PV electricity and higher heat

losses from the store and from the pipes. However, SSR_{sys} is increased to 32 %, and $W_{el,sys,grid}$ is reduced by 13 % compared to System B with the control "Standard" and by almost 25 % compared to the reference system. This means that according to the simulation results the project objective of 25 % lower grid electricity can already be reached with System B and this control strategy.

SCR is increased from 21 to 34 %, as PV feed-in into the grid is reduced by about 1100 kWh compared to strategy "Standard". Actually, grid feed-in is reduced more than grid consumption, which is a result of the higher overall electricity consumption due to overcharging of the store. However, with the assumed feed-in tariff of 0.05 €/kWh compared to a consumption price of 0.18 €/kWh the net el. costs are reduced by 65 €/a.

If the strategy "PV_{Troom}" is applied additionally, grid consumption $W_{el,sys,grid}$ can be further reduced to 3964 kWh and the self-sufficiency ratio SSR_{sys} is increased to 36 %. So the variation of the room temperature of only ± 0.5 K causes an additional decrease of grid consumption of 9 % compared to "PV_{Store}". Concerning the overall project objective a reduction of $W_{el,sys,grid}$ of about 32 % is possible compared to the reference system by applying both "PV_{Store}" and "PV_{Troom}". Compared to "PV_{Store}" electricity costs are reduced by another 57 €/a.

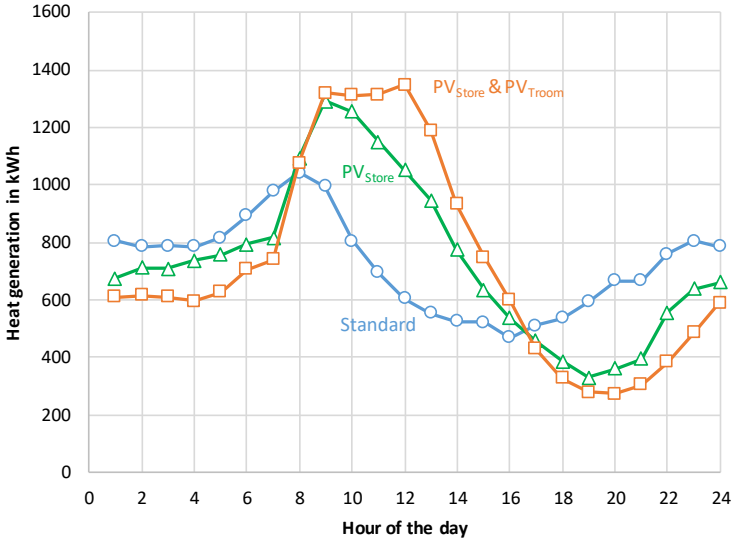

Fig. 8: Annual sum of heat generated by the HP at hours of the day with different control strategies

Both applied control strategies cause a shift of HP operation into times, where PV electricity is available, which naturally results in a shift from night to day. This can be seen in Fig. 8, which shows the annual sum of heat generated by the HP at different hours of the day for the three used strategies. On the one hand, this shift means that the HP tends to be operated with higher evaporation temperatures, as the ambient temperature is higher during the day than in the night and early morning hours. On the other hand, overcharging of the store causes higher condensation temperatures, which in the end leads to a lower SPF_{HP} compared to the strategy "Standard".

An interesting aspect about strategy "PV_{Troom}" is that the space heating demand remains almost unchanged compared to the other strategies (Fig. 6), although an adaptation of the room temperature depending on available PV excess electricity is done. The reason is that the adaption in both directions (± 0.5 K) causes the room temperature to be on average very similar to strategy "Standard". This is shown in Fig. 9 with hourly average values of the room temperature and annual duration curves of the room temperature for both strategies. Concerning thermal comfort a room temperature variation in this range should not be a problem.

A simulation variant that was carried out with only increasing the set room temperature in times of available PV (+ 1 K) showed that this also decreases the grid consumption, but to a much lower extent. This is due to an increase of the space heating demand and therefore also the overall system electricity consumption. Due to the increased consumption a larger fraction of PV electricity is consumed on site and a smaller fraction is fed into the grid. This also causes disadvantages concerning the net electricity costs compared to the here used strategy PV_{Troom}.

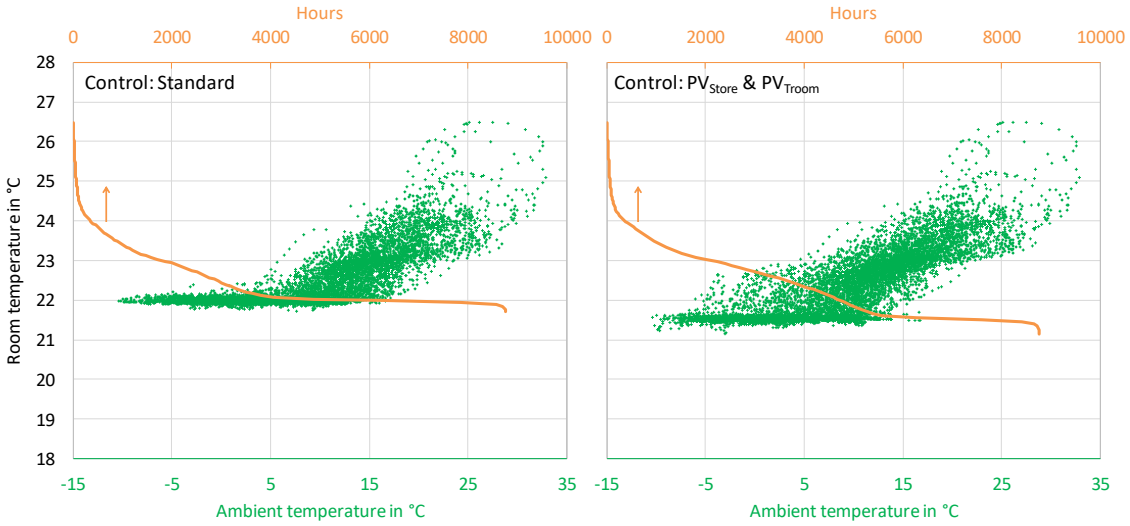

Fig. 9: Room temperatures (hourly averages) as function of the ambient temperature and annual duration curve of the room temperature for System B with the control strategies "Standard" and "PV_{Store}, PV_{Troom}"

All results presented up to here apply to the initially assumed PV capacity of 10 kWp. With this size the self-consumption ratio SCR is 37 %, so a large fraction of the PV electricity is fed into the grid. Now it would be interesting to see how the results change when a smaller PV system is used. Thus, the PV size was varied between 1 and 10 kWp to analyze the influence. The results are shown in Fig. 10 for System B with the control strategies "Standard" and "PV_{Store} & PV_{Troom}". As expected, $W_{el,sys,grid}$ and $W_{el,grid}$ increase with decreasing PV size, while $W_{el,feedin}$ decreases. However, the increase of grid consumption is much lower than the decrease of feed-in. For example, if the PV system is changed from 10 to 5 kWh, $W_{el,grid}$ increases by 620 kWh, while $W_{el,feedin}$ decreases by 3740 kWh (strategy "PV_{Store} & PV_{Troom}").

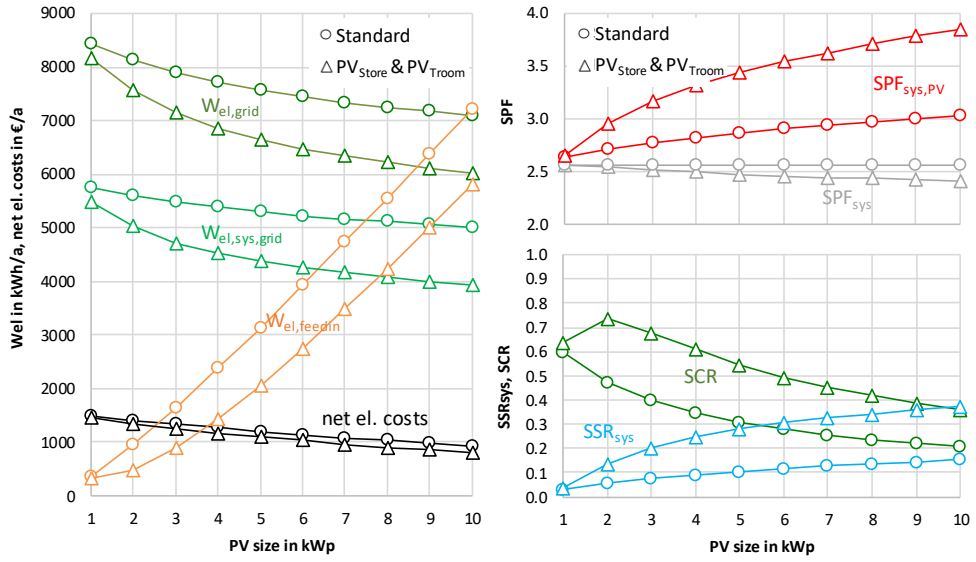

Fig. 10: Influence of the PV size on the system performance for System B with the control strategies "Standard" and "PV_{Store} & PV_{Troom}"

Decreasing the PV size results in a reduction of $SPF_{sys,PV}$, but an increase of SPF_{sys}. The latter is because a larger amount of available PV electricity leads to increased overcharging of the store and therefore higher overall electricity consumption. For strategy "Standard" SPF_{sys} is independent of the PV size, as here HP and PV are operated "in parallel" without interaction.

The self-consumption ratio SCR increases with decreasing PV size, with a maximum of 74 % at 2 kWp. With the smallest size of 1 kWp, SCR decreases, which is mostly due to the criterion for switching on the PV overcharging

(see section 2.7), which is hardly reached with this very small size. The maximum self-sufficiency ratio SSR_{sys} of 37 % is achieved with the largest PV size, but in this case with a SCR of only 36 %.

5 Conclusions and Outlook

The results of the performed analysis show that a hybrid system combining an air-source heat pump with PV is a possibility to significantly reduce the electricity consumption and the operative costs of the considered heating system in a renovated building with high supply temperatures and a heating demand (space heating and DHW) of about 15200 kWh.

With the shown combination of a dedicated HP, optimized integration of a combistore and targeted operation of the HP with electricity from a 10 kWp PV system, a reduction of the electricity consumption from the grid of 32 % compared to a reference system with the same PV size is possible. If only electricity from the grid is considered, the system seasonal performance factor ($SPF_{sys,PV}$) is 3.8, which is in the range of a ground source HP in combination with a low-temperature heating system.

Using a heat pump in combination with a low-temperature heating system should of course always be preferred and could achieve even better overall results if combined with PV. However, current market practice shows that existing high-temperature systems are often not replaced during renovations and here a combination with PV is an attractive solution to significantly save energy, CO_2 emissions and costs.

The net electricity costs (considering also PV electricity sold to the grid) of the proposed system are 264 €/a lower than for the reference system, assuming an electricity purchase price of 0.18 €/kWh and a feed-in tariff of 0.05 €/kWh. Compared to the reference system without any PV the cost savings are 946 €/a. Assuming investment costs for a PV system in the range of 1300 to 1700 €/kWp the PV installation should pay off well within the lifetime.

One noteworthy aspect about the results is that the project objective of 25 % reduction of grid consumption of the system can easily be achieved also with a smaller PV size. With only 5 kWp -24.8 % are possible compared to the reference system, for which a PV size of 10 kWp was assumed. Compared to a reference system without any PV the reduction is 35 %. A smaller size could be especially interesting due to the larger fraction of electricity consumed on-site, as feed-in tariffs are likely to further decrease in the future.

The main components of the proposed system have already been tested in the laboratory of IWT (heat pump) and SPF (storage tank), whereby the results of these measurements were considered in the parametrization of the used simulation models. The complete hybrid heating system is currently assembled at SPF in Rapperswil, where it will be tested in a 6-day Hardware-in-the-Loop system test, which enables an extrapolation to annual results. The aim of this test is to confirm the results of the simulation work carried out within the project and the calculated performance figures.

6 Acknowledgments

The project “HybridHeat4San” is funded by the Austrian Climate and Energy Fund and is carried out as part of the Energy Research Program 2016.

7 References

Amtmann M. (2010): ‘Scientific Report D6.9: Reference buildings - The Austrian building typology, A classification of the Austrian residential building stock. IEE - Intelligent Energy Europe.’ Österreichische Energieagentur – Austrian Energy Agency, 2010.

Bales C., Heinz A., and Haller M. (2012): ‘Deliverable 7.1 - Definition of Boundary Conditions, FP7 project MacSheep (grant agreement 282825)’, 2012.

Battaglia M., Haberl R., Bamberger E., Haller M. (2017): ‘Increased self-consumption and grid flexibility of PV and heat pump systems with thermal and electrical storage’, Energy Procedia, vol. 135, pp. 358–366, Oct. 2017.

Biberacher M. (2010): ‘Räumliche Modelle als Entscheidungsgrundlage für die Inwertsetzung regional verfügbarer Energiepotenziale zur CO_2-neutralen Deckung des lokalen Wärmebedarfs’, 2010.

Dott R., Haller M. Y., Ruschenburg J., Ochs F., Bony J., 2013: 'The reference framework for system simulations of the IEA SHC Task 44/HPP Annex 38 Part B: buildings and space heat load', International Energy Agency, 2013.

Dott R., Afjei T., Genkinger A., Dalibard A., Carbonell D., Consul R., Heinz A., Haller M., Witzig A., Facão J. (2013): Models of sub-components and validation for the IEA SHC Task 44/HPP Annex 38 Part C: heat pump models. International Energy Agency, A technical report of subtask C Deliverable C 2.

Drück H. (2006): „MULTIPORT Store-Model for TRNSYS, Type340. Version 1.99F, March 2006". 2006.

EC (2013): 'Commission Delegated Regulation (EU) No 812/2013 of 18 February 2013 supplementing Directive 2010/30/EU of the European parliament and of the Council with regard to the energy labelling of water heaters, hot water storage tanks and packages of water heater and solar device'. 06-Sep-2013; https://eur-lex.europa.eu/legal-content/DE/TXT/PDF/?uri=OJ:L:2013:239:FULL&from=DE.

Haberl R., Schmidli J., Heinz A., Kalkgruber J. & Haller M.Y. (2020): A Combi Storage for Combination with Heat Pumps - From Simulations to the Test Bench Results. In: Proc. of the EuroSun 2020 Conference, Athens, Greece.

Haller H. (2007): 'Type 805: DHW heat exchanger, Version 1.1', SPF Institute for Solar Technology, 2007

Haller M.Y., Haberl R, Persdorf P, Reber A. (2018): Stratification Efficiency of Thermal Energy Storage Systems – A new KPI based on Dynamic Hardware in the Loop Testing - Part I: Test Procedure. Energy Procedia 2018;155:188–208. https://doi.org/10.1016/j.egypro.2018.11.056.

Haller MY, Haberl R, Reber A. (2019): Stratification efficiency of thermal energy storage systems – A new KPI based on dynamic hardware in the loop testing - Part II: Test results. Energy and Buildings 2019;202:109366. https://doi.org/10.1016/j.enbuild.2019.109366.

Hengel F., Heinz A., Rieberer R. (2014): Analysis of an air source heat pump system with speed controlled compressor and vapor injection; in: 11th IEA Heat Pump Conference., pp. 1–15.

Jordan U., Vajen K. (2012): 'DHWcalc - Tool for the Generation of Domestic Hot Water (DHW) Profiles on a Statistical Basis'. Universität Kassel, Institut für Thermische Energietechnik, 2012.

LoadProfileGenerator (2018). [Online]. Available: http://www.loadprofilegenerator.de/. [Accessed: 07-Mar-2018].

NTB Buchs (2018): Prüfresulate Wärmepumpen; NTB Buchs, Institut für Energiesysteme IES - Wärmepumpen Testzentrum WPZ. Available online: https://www.ntb.ch/fue/institute/ies/wpz/pruefresultate-waermepumpen/. [accessed: 06-Feb-2018].

Pflugradt N. D. (2016): 'Modellierung von Wasser- und Energieverbräuchen in Haushalten', Dissertation, Technische Universität Chemnitz, 2016.

Schramek E. R., Recknagel H. (2007): "Taschenbuch für Heizung + Klimatechnik 07/08". Oldenbourg Industrieverlag, ISBN 10: 3-8356-3104-7, 2007

Tabula (2018): 'TABULA WebTool'. [Online]. Available: http://webtool.building-typology.eu/?c=all#bm. [Accessed: 31-Jan-2018].

Thür A., Calabrese T., Streicher W. (2018): 'Smart grid and PV driven ground heat pump as thermal battery in small buildings for optimized electricity consumption', Solar Energy, vol. 174, pp. 273–285, Nov. 2018.

Toradmal A., Kemmler T., Thomas B. (2018): 'Boosting the share of onsite PV-electricity utilization by optimized scheduling of a heat pump using buildings thermal inertia', Applied Thermal Engineering, vol. 137, pp. 248–258, Jun. 2018.

TRNSYS (2014): „TRNSYS 17: a Transient System Simulation Program, Volume 4: Mathematical Reference. Solar Energy Laboratory, University of Wisconsin-Madison". 2014.

TRNSYS 17 (2014): „TRNSYS 17: a Transient System Simulation Program, Volume 4: Mathematical Reference. Solar Energy Laboratory, University of Wisconsin-Madison". 2014.